

Atomic-force and scanning tunneling microscopy study of Langmuir–Blodgett films of comb-shaped liquid-crystal polymer: molecular lattice, induced conductivity, and charge superstructure

N. S. Maslova, Yu. N. Moiseev, V. I. Panov, S. V. Savinov, and D. A. Znamenskii¹⁾

M. V. Lomonosov Moscow State University

(Submitted 6 November 1991)

Zh. Eksp. Teor. Fiz. **102**, 925–933 (September 1992)

Langmuir–Blodgett films of a liquid-crystal comb-shaped polymer PKhA-10 were investigated by the methods of scanning tunneling microscopy (STM), scanning tunneling spectroscopy (STS), and atomic-force microscopy (AFM). The structure of the molecular surface lattice of a bilayer film was determined from the AFM images. The STS and STM methods revealed the existence of tunneling conductivity induced by the tunneling microscope tip and making it possible to observe the atomic structure of the graphite substrate under a layer of film about 66 Å thick. In the current mode of the STM image, a superstructure depending on the sign of the tunneling voltage and indicating the existence of a distributed surface charge of the charge-density-wave type, was observed on the film. Models of the observed effects are proposed and discussed.

1. INTRODUCTION

In the last few years films of liquid crystals (LCs) have been under intensive study by different methods.^{1,2} Scanning tunneling microscopy (STM), scanning tunneling spectroscopy (STS), and atomic-force microscopy (AFM), which make it possible to study the structural and electrophysical properties of materials on atomic scales, occupy a significant place among these methods.

Films of liquid crystals are of interest because of new effects which have been discovered in them and the possibility of developing on their basis quantum-tunneling systems and nanometer-size devices for electronic and optical technology and for information processing.

For this reason, in the present work we employed the methods of AFM, STM, and STS to investigate monolayers of a liquid-crystalline polymer, which at room temperatures forms a smectic phase. With the help of an atomic-force microscope we observed, on the surface of a bilayer of a Langmuir–Blodgett film (LB) of a comb-shaped polymer, a two-dimensional molecular lattice with edges $a_1 \approx a_2 = 11.9$ Å and short diagonal $d_1 \approx 10.9$ Å.

In the AFM image of the molecular lattice of this bilayer CH₃ groups, separated by a distance of 5.4 Å, were clearly resolved for each lattice site. This indicates that Y layers are formed in the LB film.

With the help of the STM and STS methods we observed conductivity induced by the tunneling microscope tip in the experimental films of this polymer, which exhibits dielectric properties in bulk samples.

The tunneling conductivity which we observed is associated with the change in the height of the effective barrier in the substrate–liquid crystal–barrier–tip system, as a result of which we were able to observe in the current STM image the atomic structure of graphite under an approximately 66 Å thick film of the liquid crystal.

Large-scale periodic structure was observed in the current mode of the STM images of the surface of the liquid crystal. The phase of the image of the structure changes when the sign of the tunneling voltage U_t changes. The

structure indicates the existence of distributed surface charge of the charge-density-wave type on the surface of the liquid crystal. In order to explain the experimental results, models of the effects which we observed are proposed and discussed in the paper.

2. MATERIALS AND MEASUREMENT PROCEDURE

The experimental material consisted of liquid-crystalline cholesteric comb-shaped polymer (Fig. 1), which in the temperature range 10 °C–100 °C forms a smectic phase. Films of this polymer were deposited on a substrate consisting of highly oriented pyrolytic graphite (HOPG) and silicon ([100] plane) by the Langmuir–Blodgett method. The bilayer studied was formed under a surface pressure of about 30 dynes/cm and was deposited on the substrates immediately after the substrates were cleaned.

The surface structure of the bilayer of the liquid crystal and the tunneling through the layer were investigated with the help of a scanning tunneling microscope and an atomic-force microscope with a tunneling displacement sensor.³ The AFM investigations were conducted in the repulsive potential regime with an interaction force of 10^{-8} N between the tip and the surface. The STM and AFM measurements were performed on the instrument with a resolution of ~ 0.1 Å along the normal to the surface. The STM tip consisted of a PtIr needle, prepared by the mechanical cutting method.

3. RESULTS

The initial investigation of the surface topography of the bilayer of the liquid crystal was conducted with the help of an AFM at the temperature 20 °C under atmospheric conditions. For the film parameters presented above, an image with a pronounced two-dimensional lattice, having edges $a_1 \approx a_2 = 11.9$ Å and short diagonal $d_1 \approx 10.9$ Å (Figs. 2a, b), was obtained. In addition, one can see on the obtained AFM image that each site of the surface lattice consists of two pronounced bulges of atomic size. The bulge tops, which are separated by a distance of 5.4 Å, correspond to an arrangement in which the CH₃ groups for the hydrophobic

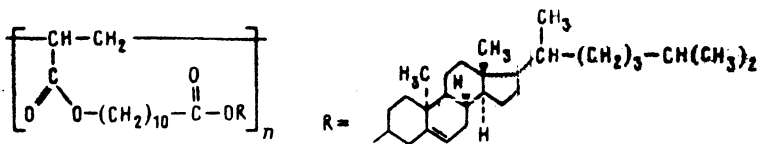


FIG. 1. Structural formula of the liquid-crystal comb-shaped polymer PKhA-10.

ends of the PKhA-10 molecules are located in the *Y*-type bilayer formed on the substrate.

In the STM experiments we investigated the surface topography at $I_t = \text{const}$, the surface topography at $z = \text{const}$ (current images), the current as a function of the distance between the needle and the sample $I_t(\Delta z)$, and the current-voltage characteristics (IVC) $I_t(U)$.

The $I_t(\Delta z)$ dependence was recorded as follows: The values of the tunneling current I_{t0} and the tunneling voltage U_{t0} , corresponding to the initial gap, were determined, after which the electronic feedback circuit controlling the vertical displacement of the STM needle was disconnected. Next, the value of the current I_t was recorded with decreasing distance z between the tip and the graphite surface. The curve $I_t(\Delta z)$ was constructed using 100 points, in each of which the value of the current I_t was obtained by averaging over 10 measurements with the same value of z . The time required to obtain such a curve was equal to about 0.3 s. An analogous method was used to obtain the IVC $I_t(U)$. In order to assess the influence of instrumental effects, the dependence $I_t(\Delta z)$ [or $I_t(U)$] was measured with constant z (or U_t). In the process, the tunneling current varied by not more than 0.1 nA.

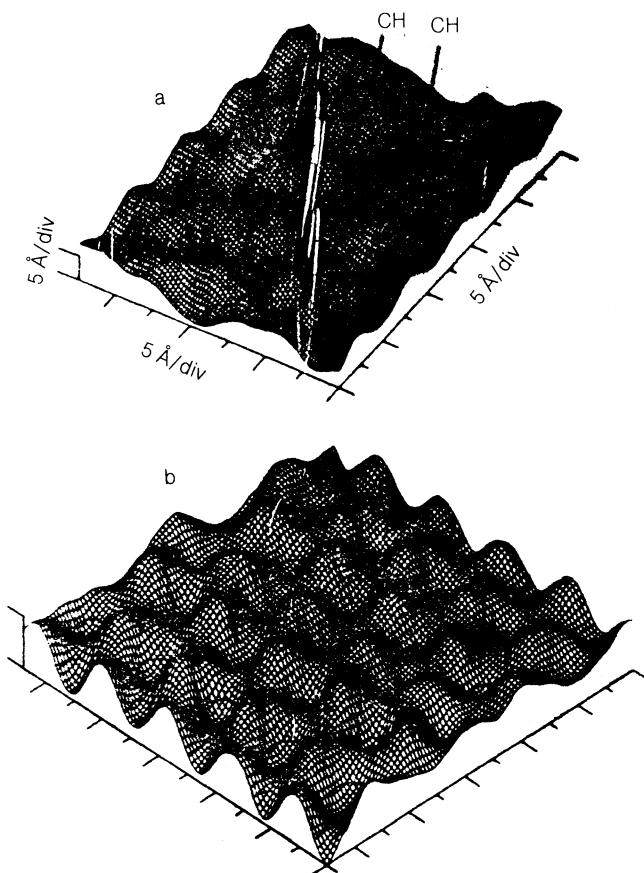


FIG. 2. a, b) AFM image of the molecular surface lattice of a PKhA-10 bilayer.

Preliminary measurements of the surface structure of HOPG demonstrated a typical defect-free image of the atomic lattice in the current and topographic modes of the STM. We obtained two types of IVCs for the graphite-liquid crystal-barrier-tip system. For large distances, a quite wide (~ 5 eV) forbidden region [Fig. 3 (1)] containing Fermi level E_F and indicating that under these conditions the liquid crystal-adsorbate system has a low conductivity of $\sigma \sim 10^{-9}$ S, was observed in the IVC. As the initial voltage increases (the needle approaches the surface of the liquid-crystal film) the conductivity increases by two orders of magnitude to $\sigma \sim 10^{-7}$ S [Fig. 3 (2)].

For conditions under which the liquid-crystal film exhibits tunneling conductivity, we obtained current images of the liquid crystal with positive and negative potentials on the tip (Figs. 4a, b). A periodic superstructure, corresponding to a lattice with the parameters $a_1 \approx a_2 \approx 25$ Å and $d_1 \approx 20$ Å, significantly exceeding the lattice parameters which were observed in the AFM image, can be seen in these current images. One can see from the figures that when the sign of the tunneling voltage is reversed the phase of the image of the large-scale lattice changes. This assertion is illustrated in Fig. 5, which shows sections of the surfaces shown in Fig. 4 for the same location of the superstructure but with the opposite signs of the applied voltage. In addition, a periodic structure which has a significantly shorter period and whose phase, to within the accuracy of the measurements, is independent of the sign of the voltage on the tip, is observed in the images obtained. This small-scale structure, manifesting in the STM image on the surface of the liquid crystal, corresponds to the surface lattice of graphite located underneath the 66 Å thick layer of the liquid crystal.

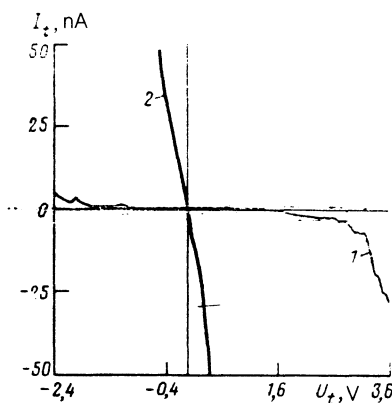


FIG. 3. Current-voltage characteristics of a PKhA-10 bilayer on graphite for two tip-surface distances corresponding to the initial parameters $I_0 = 0.8$ nA and $U_0 = 1.5$ V (curve 1) and $I_0 = 0.8$ nA and $U_0 = 5$ mV (curve 2).

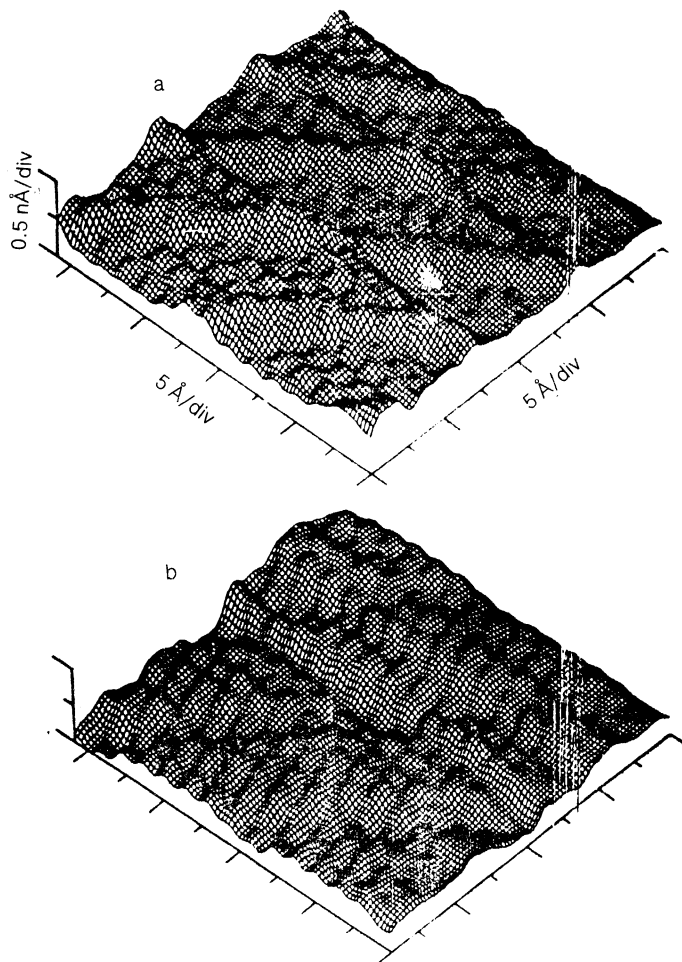


FIG. 4. STM images of the charge superstructure. The images were obtained in a regime of constant height $U_t = +5$ mV (a) and $U_t = -5$ mV (b).

4. DISCUSSION

The presence of large-scale periodic structure in the STM image and the dependence of the phase of this structure on the polarity of the applied voltage indicate that a charge density wave can exist on the surface of the liquid-crystal film. Indeed, the CH_3 groups on the surface of the liquid crystal form a simple skewed lattice with basis vectors \mathbf{a}_1 and \mathbf{a}_2 and characteristic dimensions $|\mathbf{a}_1| = |\mathbf{a}_2| = a \approx 11.9 \text{ \AA}$

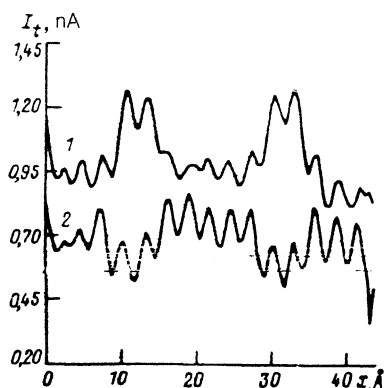


FIG. 5. Section of the images presented in Fig. 4 for the same section of the superstructure. Curve 1: $U_t = +5$ mV; curve 2: $U_t = -5$ mV.

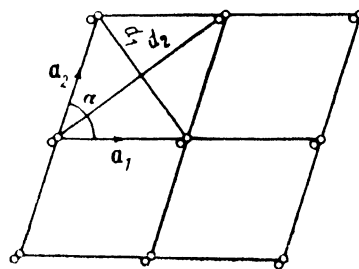


FIG. 6. Schematic diagram of the molecular lattice of the PKhA-10 bilayer. $|\mathbf{a}_1| = |\mathbf{a}_2| \approx 11.9 \text{ \AA}$, $|\mathbf{d}_1| \approx 10.9 \text{ \AA}$, $|\mathbf{d}_2| \approx 20 \text{ \AA}$.

and $|\mathbf{d}_1| \approx 10.9 \text{ \AA}$ (see Fig. 6). Electrons on the surface of the liquid crystal are located in an effective periodic potential produced by the atoms of the CH_3 groups. In the simplest strong-coupling model, in which only the interaction with the nearest sites along the directions \mathbf{a}_1 and \mathbf{a}_2 is considered, the dispersion relation for electrons on the surface of the liquid crystal can be represented in the form

$$\begin{aligned} \varepsilon(\mathbf{K}) &= t(\cos(\mathbf{K}\mathbf{a}_1) + \cos(\mathbf{K}\mathbf{a}_2)) \\ &= t(\cos(K_x a) + \cos(K_x a \cos \alpha + K_y a \sin \alpha)), \end{aligned} \quad (1)$$

where t is the transition matrix element and α is the angle between \mathbf{a}_1 and \mathbf{a}_2 (Fig. 6).

The Fermi level E_F on the surface of the liquid crystal is determined by the condition $\varepsilon(\mathbf{K}) = 0$, i.e.,

$$\begin{aligned} K_y &= \frac{\Pi}{a \sin \alpha} - K_x \operatorname{ctg} \frac{\alpha}{2}, \\ K_y &= \frac{\Pi}{a \sin \alpha} - K_x \operatorname{tg} \frac{\alpha}{2}. \end{aligned} \quad (2)$$

The basis vectors of the reciprocal lattice \mathbf{g}_1 and \mathbf{g}_2 , the surface Brillouin zone (BZ), and the position of the Fermi level are shown in Fig. 7. It is easy to see that in the model adopted "nesting" occurs in the directions \mathbf{Q} and \mathbf{m} , where the direction \mathbf{Q} coincides with the direction \mathbf{d}_2 corresponding to the

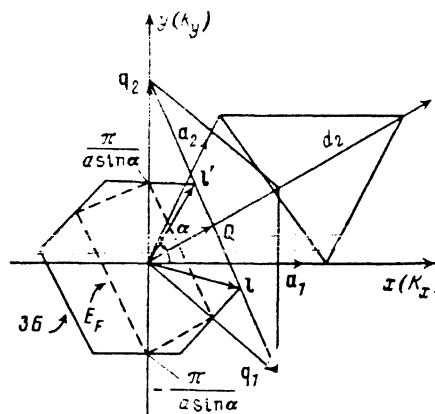


FIG. 7. Surface Brillouin zone and the position of the Fermi level for the lattice shown in Fig. 6.

$$\begin{aligned} \mathbf{a}_1 &= \begin{pmatrix} 1 \\ 0 \end{pmatrix} a, \quad \mathbf{q}_1 = \begin{pmatrix} 1 \\ -\operatorname{ctg} \alpha \end{pmatrix} \frac{2\pi}{a}, \quad \mathbf{a}_2 = \begin{pmatrix} \cos \alpha \\ \sin \alpha \end{pmatrix} a, \quad \mathbf{q}_2 = \begin{pmatrix} 0 \\ \sin \alpha \end{pmatrix} \frac{2\pi}{a}, \\ \mathbf{Q} &= \frac{\pi}{a \cos \alpha/2} \end{aligned}$$

long diagonal of the direct lattice and the direction \mathbf{m} can change from \mathbf{l} to $-\mathbf{l}$ (see Fig. 7). As a result, the general susceptibility $\chi(\mathbf{K}, \mathbf{0})$ acquires a singularity at

$$\mathbf{K} = \{\mathbf{Q}, \mathbf{m}\}.$$

In the presence of electron-phonon and interelectron interactions this singularity can result in the appearance of charge density waves in the directions \mathbf{Q} and \mathbf{m} with characteristic periods $2\pi/|\mathbf{Q}|$ and $2\pi/|\mathbf{m}|$. It should be noted that

$$(\mathbf{Qd}_2) = 2\pi,$$

i.e., the period of the charge density wave in the direction \mathbf{d}_2 is equal to $|\mathbf{d}_2|$ —the length of the long diagonal of the direct lattice. When a charge density wave forms, the Fermi level lies in the energy gap, whose width depends on the strengths of the electron-phonon and interelectron interactions.

The large-scale periodic structure obtained in the experiment has characteristic periods of 25.5 and 20.2 Å in the \mathbf{m} and \mathbf{Q} directions, respectively. The period in the \mathbf{Q} direction, falling within the spread of the experimental results, is equal to the length of the long diagonal of the direct lattice formed by the CH_3 groups. Thus there are grounds for asserting that the large-scale periodic structure observed in the STM image corresponds to a charge density wave on the surface of the liquid crystal. In addition, it is necessary to make more precise the conditions under which a charge density wave can be observed at room temperature ($kT \sim 25$ meV) and with a tunneling voltage of ~ 5 mV. In order for a charge density wave to exist the energy gap must exceed kT , because otherwise the thermal fluctuations will obliterate the charge density wave. For this reason, in the absence of an interaction of the electronic states of the STM tip and the sample it would be impossible to observe a charge density wave under such conditions.

It should be noted that bound localized states, lying significantly below E_F , can exist on the surface of the tip or the liquid crystal. These states could be due, for example, to an adsorbate, an oxide layer on the tip, impurities, or non-uniformities. As a result of the strong hybridization of the electronic states of the sample and the tip or impurity states associated with the adsorbate, a collective state forms in the gap (a similar situation also occurs in superconductors⁷). This bound state arises as a pole in the electronic Green's function (GF):

$$G(\omega, k) \sim \frac{1}{\omega - E_d - V^2 \sum_k (\omega - E_k + i\tau)^{-1}},$$

where E_d is the energy of the localized state of the tip, E_k is the spectrum of surface electrons of the liquid crystal, and V is the interaction of the tip and the surface of the sample. For a quasi-one-dimensional density of states (which corresponds to a charge density wave) the position of this level relative to the band limit and the Fermi energy E_F is determined by the degree of hybridization:

$$\bar{E} - E_v \sim \left(\frac{V^2}{E_v - E_d} \right)^2 \frac{1}{\Delta},$$

where E_v is the limit of the continuous spectrum and Δ is the effective width of the allowed band.

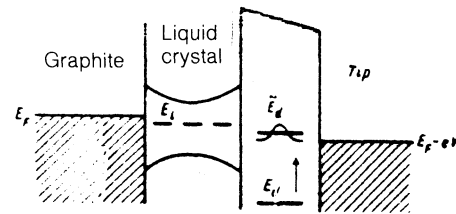


FIG. 8. Band structure of the graphite-liquid crystal-barrier-tip system, where E_F is the Fermi level, E_L is the system of resonance levels, E_d is the energy of the localized state of the tip, and \bar{E}_d is the energy of the collective bound state.

The appearance of such a state is made possible by a feature appearing, due to the presence of the charge-density wave, in the electron density of states on the surface of the liquid crystal: If at the limit of the spectrum the density of states

$$\rho_k(\omega) = 0,$$

then the Green's function has a pole at

$$\omega = \bar{E}_d,$$

lying in the gap. This situation is shown in Fig. 8, where the molecular levels of the liquid-crystal film, which form a system of intermediate states for tunneling of electrons from the graphite into the tip, are also shown.

Thus, in our opinion, the possibility of observing a charge density wave at room temperatures and $U_t = 5$ mV is related with the formation of a collective electron state in the gap against the background formed by the charge density wave.

The appearance of the STM image of graphite underneath the 66 Å thick liquid crystal layer is most likely due to resonance tunneling through the molecular and impurity levels of the liquid-crystal film. In addition, the tunneling current as a function of the change in the gap width $I_t(\Delta z)$, as shown in Fig. 9, confirms the fact that the needle is located above the liquid-crystal film. The gap of the order of 5 eV, appearing in the IVC in the absence of an image of the liquid crystal and the charge-density wave, is related, in all probability, with the presence of a dielectric adsorbate on the surface of the liquid crystal.

5. CONCLUSIONS

It should be noted that the Langmuir-Blodgett bilayers of the liquid crystal, which were studied in the present work,

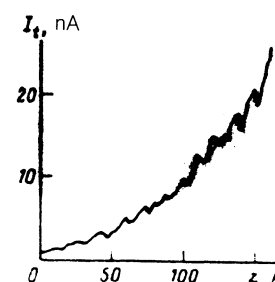


FIG. 9. Tunneling current $I_t(\Delta z)$ versus the change in the tip-sample distance with $U_0 = 15$ mV and $I_0 = 0.8$ nA.

can have different ordering of the molecular lattice. We observed this in preliminary investigations performed with the help of an AFM with atomic resolution.⁴ In addition, the effects of the appearance of a charge superstructure on the surface of the liquid crystal manifest only with a definite surface lattice of the bilayer. Induced conductivity appeared for other forms of ordering of the bilayer, but a charge superstructure was not observed in our experiments.

We sincerely thank L. V. Keldysh for his encouragement and for a fruitful discussion of the results.

¹⁾All-Union Scientific-Research Institute of TsPV.

¹D. P. E. Smith, H. Horber, C. Gerber, and G. Binnig, *Science* **245**, 43 (1989).

²N. A. Plate [Ed.], *Liquid-Crystalline Polymers* [in Russian], Khimiya, Moscow, 1988, p. 245.

³Yu. N. Moiseev, V. M. Mostepanenko, I. Yu. Sokolov, and V. I. Panov, *Phys. Lett. A* **132**, 354.

⁴Yu. N. Moiseev, V. I. Panov, S. V. Savinov *et al.*, *International Symposium on Scanning Tunneling Microscopy*, Interlaken, 1991, p. 240.

⁵P. Arseev and B. Volkov, *Solid State Commun.* **78**, 373 (1991).

Translated by M. E. Alferieff